Macromolecules
ARTICLE

Macromolecules **2010**, *43*, 4889–4901 **4889**
DOI: 10.1021/ma1005843

"Core-First" Synthesis of Multiarm Star Polyethylenes with a Hyperbranched Core and Linear Arms via Ethylene Multifunctional "Living" Polymerization with Hyperbranched Polyethylenes Encapsulating Multinuclear Covalently Tethered Pd-Diimine Catalysts

Xuewei Xia,[†] Zhibin Ye,*[,†] Shawn Morgan,[†] and Jianmei Lu[‡]

[†]*School of Engineering, Laurentian University, Sudbury, Ontario P3E 2C6, Canada, and*
[‡]*College of Chemistry and Chemical Engineering, Suzhou University, Suzhou, Jiangsu, 215123, China*

Received March 16, 2010; Revised Manuscript Received April 30, 2010

ABSTRACT: We demonstrate in this paper the novel synthesis of multiarm star polyethylenes of well-defined arm lengths and controllable average arm numbers through the core-first multifunctional "living" polymerization protocol from ethylene stock. These novel star polymers are featured with a core−shell structure, having a hyperbranched polyethylene core joining multiple linear polyethylene arms bearing short branch structures. Utilizing the outstanding features of cationic Pd−diimine catalysts, a three-step synthesis procedure incorporating two sequential Pd−diimine catalyzed ethylene polymerization steps is employed. Hyperbranched polyethylenes bearing different numbers of pendant acryloyl groups (HPE1 and HPE2) were first synthesized with an acetonitrile Pd−diimine catalyst (**2**) by nonliving chain walking copolymerization of ethylene with 1,4-butanediol diacrylate at elevated concentrations. These two hyperbranched polymers having the specific acryloyl anchoring sites were used as the homogeneous support in the second step for the covalent immobilization of catalyst **2** to generate hyperbranched polyethylenes encapsulating multinuclear covalently tethered Pd−diimine catalysts (HPE-Pd-1 and HPE-Pd-2). Acting as the multifunctional initiating hyperbranched core in the third step, the two multinuclear hyperbranched Pd catalysts initiated and catalyzed successfully ethylene multifunctional "living" polymerization at 400 psi and 5 °C, and led to simultaneous multidirectional arm growth from the hyperbranched core to form two sets of star polymers of very high molecular weights (SPE1 and SPE2 sets, respectively, with number-average molecular weight M_n up to 1,379 kg/mol). The arm growth catalyzed by the tethered Pd centers in the polymerization is confirmed to be "living", with M_n of both star polymers and the arms increases nearly linearly with polymerization time. Determined essentially by the average numbers of tethered acryloyl groups in HPE1 and HPE2, high average arm numbers (about 21 and 28 per star, respectively) were achieved in the star polymers, along with narrow-distributed tunable arm length (up to about 48 kg/mol). Study on dilute solution properties of these two sets of star polymers confirms their spherical chain conformation and resemblance of rigid spheres and high-generation dendrimers.

Introduction

Star polymers containing multiple arms joined at a central core have received extensive research attention in the past decade due to their unique three-dimensional architecture and superior properties. Resembling dendrimers and hyperbranched polymers, star polymers exhibit highly compact nanoscale globular structures with tunable inner and peripheral groups, which gives rise to their desired properties including high solubility, low melt, and solution viscosities.[1] These outstanding structural and performance features have stimulated their novel applications in various areas, including compartmented catalysis,[2] drug delivery,[3] rheology modification,[4] coating,[5] etc. Synthesis of star polymers, particularly those of well-defined arm length and number, is often accomplished with the use of "living" or controlled polymerization techniques.[1,6−10] Classical "living" anionic[6] and cationic[7] polymerization techniques have been traditionally employed for their synthesis. Meanwhile, "living" ring-opening polymerization[8] and ring-opening metathesis polymerization[9] have also been used. The recent developments in "living"/controlled radical polymerization techniques have further expanded tremendously the scope and flexibility in their synthesis, with a great variety of well-defined star polymers successfully synthesized from different monomer stocks, including styrenics, methacrylates, and acrylates.[10]

With the "living" polymerization techniques, three synthesis strategies-"arm-first", "core-first", and "coupling-onto"-are often adopted. The "arm-first" strategy involves the preparation of "living" polymer arms and their subsequent cross-linking with a divinyl monomer while, in the "coupling-onto" strategy, the preformed reactive polymer arms are attached onto a multifunctional coupling agent. The "core-first" strategy requires specifically the use of multifunctional initiators capable of initiating simultaneous, multidirectional "living" growth of polymer arms from multiple initiating sites bound on the central core. Compared to the other two strategies, the "core-first" strategy has the advantage of offering a more precise control over arm number by tailoring the number of functionality of the multifunctional initiators.[1,6−10] A variety of multifunctional initiators have been successfully developed to suit each of the above "living" polymerization techniques for "core-first" synthesis of star polymers from various monomer stocks. Because of their high and controllable number of functionality, multifunctional dendritic initiators (i.e., dendrimer and hyperbranched polymers bearing multiple initiating sites) are particularly valuable for synthesis of star polymers having high tunable arm numbers (as high as 20 and higher).[8c−f,9c,10h−j]

*Corresponding author. E-mail: zye@laurentian.ca. Fax: 1(705) 675-4862.

Published on Web 05/07/2010

Scheme 1. Structure of Trinuclear Pd−Diimine Catalyst (1), Acetonitrile Pd−Diimine Catalyst (2), and Mononuclear Pd−Diimine Ester Chelate Catalyst (3)

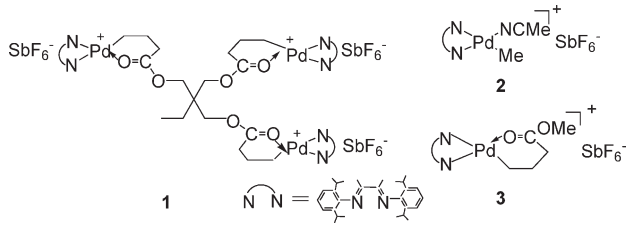

Synthesis of star polyolefins from olefin monomer stocks (like ethylene) using catalytic "living" olefin coordination polymerization technique, however, has lagged behind tremendously in sharp contrast to the great success achieved with other types of "living"/controlled polymerization techniques. This "living" polymerization technique has rarely been developed yet for synthesis of star polymers though it has advanced significantly in the past decades with a number of well-behaved transition metal catalysts developed.[11] While there are several comb-shaped polyolefins with star-like conformations synthesized in the literature via macromonomer polymerization, these reported polymers are not true star polymers and/or their synthesis does not involve "living" coordinative olefin polymerization.[12] With specific regard to the "core-first" strategy for star polyolefins, the underlying challenge lies in the tremendous difficulty in finding multinuclear metal catalysts which bind multiple metal centers capable of initiating multidirectional "living" coordinative chain growth from a common central core.[13]

To this end, our group has recently discovered the first multinuclear catalyst, a trinuclear Pd−diimine chelate catalyst (**1** in Scheme 1), which facilitates unprecedentedly "core-first" synthesis of three-arm symmetrical star polyethylenes via ethylene "living" polymerization.[13] Catalyst **1** has three identical 6-membered cationic Pd chelate centers bound together at the triester core. With each Pd chelate center being readily active to catalyze "living" chain growth from the Pd−CH_2 initiating site, catalyst **1** has been demonstrated to simultaneously initiate the three-directional "living" chain growth emanating from the triester core at 400 psi (ethylene pressure) and 5 °C, and lead to well-defined three-arm symmetric star polyethylenes of narrow-distributed controllable arm length after purification.[13] This novel trinuclear catalyst was synthesized conveniently in one-step by reacting a cationic acetonitrile Pd−diimine complex (**2** in Scheme 1) with a triacrylate (trimethylolpropane triacrylate) through its three acryloyl double bonds. The characteristic reaction between **2** and the acryloyl groups produces the stable 6-membered ester chelate structures.[13]

In this paper, we further report the versatile synthesis of core−shell structured multiarm star polyethylenes having much higher numbers (average about 21 and 28) of linear arms joined at a hyperbranched core from ethylene stock by using the unique "core-first" synthetic strategy through Pd-catalyzed multifunctional "living" polymerization. To achieve the high arm numbers and core−shell architecture, we have developed herein hyperbranched polyethylenes encapsulating covalently tethered Pd−diimine chelate centers at different average numbers and have used them as multinuclear initiating/catalytic core for ethylene multifunctional "living" polymerization.[14] These Pd-encapsulating hyperbranched polyethylenes are obtained by immobilizing catalyst **2** onto hyperbranched polyethylenes containing pendant acryloyl groups, which are synthesized separately through ethylene copolymerization with 1,4-butanediol diacrylate (BDA) catalyzed by catalyst **2**.[15] Successful ethylene multifunctional "living" polymerization with the homogeneous hyperbranched-polyethylene-supported Pd catalysts is demonstrated, rendering multiarm star polyethylenes having well-defined arm lengths and tunable average arm numbers. Characterization of polymer dilute solution properties with triple-detection gel permeation chromatography (GPC) confirms the highly compact spherical shaped chain conformation of this novel range of multiarm star polymers.

Experimental Section

Materials. All manipulations involving air- and/or moisture-sensitive compounds were carried out in a N_2-filled glovebox or using Schlenk technique. The acetonitrile Pd−diimine catalyst, $[(ArN{=}C(Me){-}(Me)C{=}NAr)Pd(CH_3)(N{\equiv}CMe)]^+SbF_6^-$ (Ar = 2,6-(*i*Pr)$_2$C$_6$H$_3$) (**2**), was synthesized according to a literature procedure.[16] Ultrahigh purity N_2 (>99.97%) and polymer-grade ethylene (both from Praxair) were purified by passing through 3 Å/5 Å molecular sieves and Oxiclear columns to remove moisture and oxygen, respectively, before use. Chlorobenzene (99.5%, Aldrich) was refluxed over CaH_2 (powder, 90−95%, Aldrich) and distilled before use. Other chemicals, including anhydrous dichloromethane (>99.5%), anhydrous diethyl ether (ACS, > 99%), anhydrous pentane (>99%), tetrahydrofuran (THF, ACS reagent grade), and methanol (ACS reagent grade), were obtained from Aldrich and were all used as received.

Synthesis of Hyperbranched Polyethylenes Containing Pendant Acryloyl Groups, HPE1 and HPE2. The two hyperbranched polyethylenes containing pendant acyloyl groups (HPE1 and HPE2) were synthesized in our previous work by one-step chain walking copolymerization of ethylene with BDA at elevated concentrations using catalyst **2**.[15] HPE1 was synthesized at 15 °C with an ethylene pressure of 1 atm and a BDA concentration of 0.53 M (run 9 in our previous paper).[15] HPE2 was synthesized at 25 °C with an ethylene pressure of 1 atm and a BDA concentration of 0.27 M (run 4 in our previous paper).[15] A polymerization time of 24 h was used for both polymers. Please refer to our previous paper[15] for the detailed synthesis and characterization procedures.

Synthesis of Hyperbranched Polyethylenes Encapsulating Covalently Tethered Pd−Diimine Catalysts, HPE-Pd-1 and HPE-Pd-2. HPE-Pd-1 was synthesized by immobilizing the Pd−diimine catalyst onto the hyperbranched polyethylene HPE1. A dried Schlenk flask was charged with HPE1 (0.42 g with 0.25 mmol pendant acryloyl groups), catalyst **2** (0.29 g, 0.36 mmol, 1.4 equiv), and anhydrous dichloromethane (30 mL). The orange solution was stirred for 5 days under N_2 protection. The resulting solution was filtered through a Teflon syringe filter (0.2 μm pore size) and the solvent was evaporated under vacuum. The resulting brown gel-like solid was redissolved in anhydrous diethyl ether (30 mL) and the solution was left standing still to allow the unreacted **2** to precipitate out. After filtration, the solution was dried under vacuum to remove the solvent. It was then subject to two additional dissolution−precipitation−filtration cycle. Finally, the solvent was evaporated under vacuum from the resulting solution. After further drying under vacuum at room temperature, HPE-Pd-1 (0.18 g) was obtained as a brown elastic solid.

HPE-Pd-2 was synthesized in a similar procedure with the use of HPE2. In a dried Schlenk flask, HPE2 (1.45 g, containing 0.62 mmol pendant acryloyl groups) and catalyst **2** (0.54 g, 0.67 mmol, 1.1 equiv) were dissolved with 75 mL of anhydrous dichloromethane. The orange solution was stirred for 5 days under N_2 protection. The resulting solution was filtered through a Teflon syringe filter (0.2 μm pore size) and the solvent was subsequently removed under vacuum. The resulting gel-like brown solid was redissolved in anhydrous pentane (ca. 50 mL), filtered with a syringe filter to remove unreacted **2**, and dried under vacuum. This redissolution-filtration-evaporation procedure was repeated twice. Finally, HPE-Pd-2 (1.08 g) was obtained as a brown elastic solid after drying overnight under vacuum at room temperature.

Ethylene "Living" Polymerization with HPE-Pd-1 at 400 psi and 5 °C. Ethylene "living" polymerization with HPE-Pd-1 at 400 psi and 5 °C was carried out in a 500 mL Autoclave Engineers Zipperclave reactor equipped with a MagneDrive agitator, a removable heating/cooling jacket, and a sampling port. The reactor temperature was controlled by passing a water/ethylene glycol mixture set at a desired temperature through the reactor jacket using a refrigerating/heating circulator. This polymerization system has been used in our earlier works,[13,17,18] and a similar polymerization procedure was used herein. Prior to the polymerization, the reactor was cleaned carefully using toluene and acetone, respectively. It was then heated at ca. 75 °C and was subject to several cycles of nitrogen purge−vacuum procedure. Anhydrous chlorobenzene (150 mL) was injected into the reactor under N_2 protection, followed with the injection of HPE-Pd-1 (0.18 g) dissolved in anhydrous dichloromethane (10 mL). After establishing the equilibrium temperature at 5 °C, the reactor was then quickly pressurized with ethylene to 400 psi to start the polymerization. During the course of polymerization, ethylene pressure was maintained constant at 400 psi by continuous feed of ethylene from a cylinder and the reactor temperature was controlled at 5 °C with the use of the circulator. Every hour for 6 h, a prescribed volume (about 22 mL, see below for sampling volume) of polymerization solution was sampled from the reactor through the sampling port. Each sampled solution was quickly quenched with triethylsilane (ca. 0.2 mL) under stirring. After stirred for about 2 h, each quenched solution was filtered through a syringe filter (0.2 μm pore size) to remove the decomposed Pd black, and the polymer was obtained by precipitation in a large amount of methanol. The polymer precipitate was dried using a flowing air stream and was redissolved in THF, followed with a further precipitation in methanol. This dissolution−precipitation procedure was repeated until the polymer precipitate became clear. The final polymer samples were obtained by drying the precipitates in a vacuum oven at about 60 °C overnight. These as-produced polymer samples were weighed and were characterized. Yield of as-produced polymers: 1 h, 0.11 g (sampling volume, 21.5 mL); 2 h, 0.22 g (22.0 mL); 3 h, 0.35 g (23.0 mL); 4 h, 0.51 g (26.0 mL); 5 h, 0.64 g (23.5 mL); 6 h, 0.86 g (26.5 mL).

Ethylene "Living" Polymerization with HPE-Pd-2 at 400 psi and 5 °C. A polymerization procedure similar to that given above was used for the "living" polymerization with HPE-Pd-2. The polymerization was carried out with the use of 300 mL of chlorobenzene and 0.84 g of HPE-Pd-2 dissolved in 20 mL of dichloromethane. The polymerization was also carried out for 6 h with polymerization solution sampled every 1 h. The same polymer quenching and purification procedures as above were applied. Yield of the as-produced polymers: 1 h, 0.32 g (sampling volume, 40 mL); 2 h, 1.12 g (122 mL); 3 h, 0.42 g (20 mL); 4 h, 1.33 g (68 mL); 5 h, 0.32 g (16 mL), 6 h, 1.41 g (52.5 mL).

Polymer Cleavage by Alkaline Hydrolysis. To determine molecular weight information on the polymer arms and average arm numbers, alkaline hydrolysis experiments were carried out to cleave the ester functionalities, which connect the arms to the hyperbranched polyethylene core.[13] A general hydrolysis procedure is as follows. As-produced polymer sample (ca. 0.1 g) was dissolved in THF (ca. 40 mL) in a 100 mL round-bottomed flask fitted with a condenser, followed with the addition of KOH (ca. 0.2 g) and water (ca. 2 mL). The mixture was refluxed for 36 h. It was then evaporated to dryness and redissolved in THF (ca. 10 mL) under ultrasonication. The resulting solution was filtered using a syringe filter (0.2 μm) and the cleaved polymer was precipitated out in methanol, followed with drying under vacuum at 60 °C overnight.

Characterizations and Analyses. Proton nuclear magnetic resonance (^{1}H NMR) spectra of the polymers were obtained on a Bruker AV500 spectrometer at ambient temperature with CD_2Cl_2 or $CDCl_3$ as solvent. Polymer characterizations with triple-detection gel permeation chromatography (GPC) were carried out on a Polymer Laboratories PL-GPC220 system equipped with a differential refractive index (DRI) detector (from Polymer Laboratories), a three-angle light scattering (LS) detector (high-temperature miniDAWN from Wyatt Technology), and a four-bridge capillary viscometer (from Polymer Laboratories). The detecting angles of the light scattering detector were 45, 90, and 135°, and the laser wavelength was 687 nm. One guard column (PL# 1110−1120) and three 30 cm columns (PLgel 10 μm MIXED-B 300 × 7.5 mm) were used. This system has been used extensively in our earlier works.[13,15,19] HPLC-grade THF was used as the mobile phase at a flow rate of 1 mL/min. The complete GPC system, including columns and detectors, was maintained at 33 °C. The mass of the polymers injected into the column varied with polymer molecular weight; typically 200 μL of 1.5−6 mg/mL solution was injected. Astra software from Wyatt Technology was used for data collection and analysis. Two narrow polystyrene standards (from Pressure Chemicals) with weight-average molecular weight (M_w) of 30 000 and 200 000 g/mol were used for the normalization of light scattering signals at the three angles, and the determination of interdetector delay volume and band broadening, respectively. The DRI increment dn/dc value of 0.078 mL/g was used for all polyethylene samples synthesized,[13,15,19,20] and the value of 0.185 mL/g was used for polystyrene. The two polystyrene standards were measured to have a typical M_w value of 30.2 and 202.7 kg/mol, respectively, with a polydispersity index (PDI) of 1.00 for both, which are in good agreement with the data provided from the supplier.

Purification of the as-produced polymers through GPC fractionation was carried out in the preparative mode on a Waters 2695 Separation System, equipped with a Waters 2414 DRI detector, one guard column (PL# 1110−1120), and three 30 cm columns (PLgel 10 μm MIXED-B 300 × 7.5 mm). HPLC-grade THF was used as the mobile phase at 1.0 mL/min. In each fractionation, about 100 μL of 50 mg/mL polymer solution was injected into the column. By monitoring the signals from the DRI detector, the GPC effluents corresponding to both high-molecular-weight peak and low-molecular-weight peak were collected respectively to render the high-molecular-weight fraction (purified multiarm star polymers) and the remainder as low-molecular-weight fraction. After solvent evaporation, the purified star polymers were recovered and were subsequently characterized with triple-detection GPC.

Results and Discussion

Synthesis Procedure. A three-step synthesis procedure, including two Pd−diimine catalyzed ethylene polymerization steps, is developed herein for synthesis of multiarm star polyethylenes from ethylene stock through the core-first multifunctional "living" polymerization protocol. Scheme 2 depicts schematically this synthesis procedure. This synthesis fully utilizes the three combined outstanding features of Pd−diimine catalysts for ethylene polymerization, including chain walking mechanism for polymer topology control,[20,21] capability in copolymerizing functional acrylate comonomers,[15,19a,21c,22,23] and high versatility in initiating and catalyzing ethylene "living" polymerization.[13,17,18,24] In the first step of the procedure, non-living chain walking copolymerization of ethylene (at 1 atm) with 1,4-butanediol diacrylate (BDA) at elevated concentrations is carried out with catalyst **2** to produce hyperbranched polyethylenes tethered with pendant acryloyl groups at a controlled content. In an earlier paper, we have demonstrated that, at elevated feed concentrations (much greater than the critical gelation concentration), bifunctional BDA is uniquely copolymerized predominantly in the form of pendant acryloyl groups with negligible/minimum inter- or intramolecular cross-linking structures.[15] This interesting phenomenon results from the significant reduction in the concentration ratio of the pendent acryloyl groups to monomeric acryloyl groups at elevated

Scheme 2. Three-Step Procedure for Synthesis of Multiarm Star Polyethylene (PE) with a Hyperbranched Core and Linear Arms of Branching Structure from Ethylene Stock

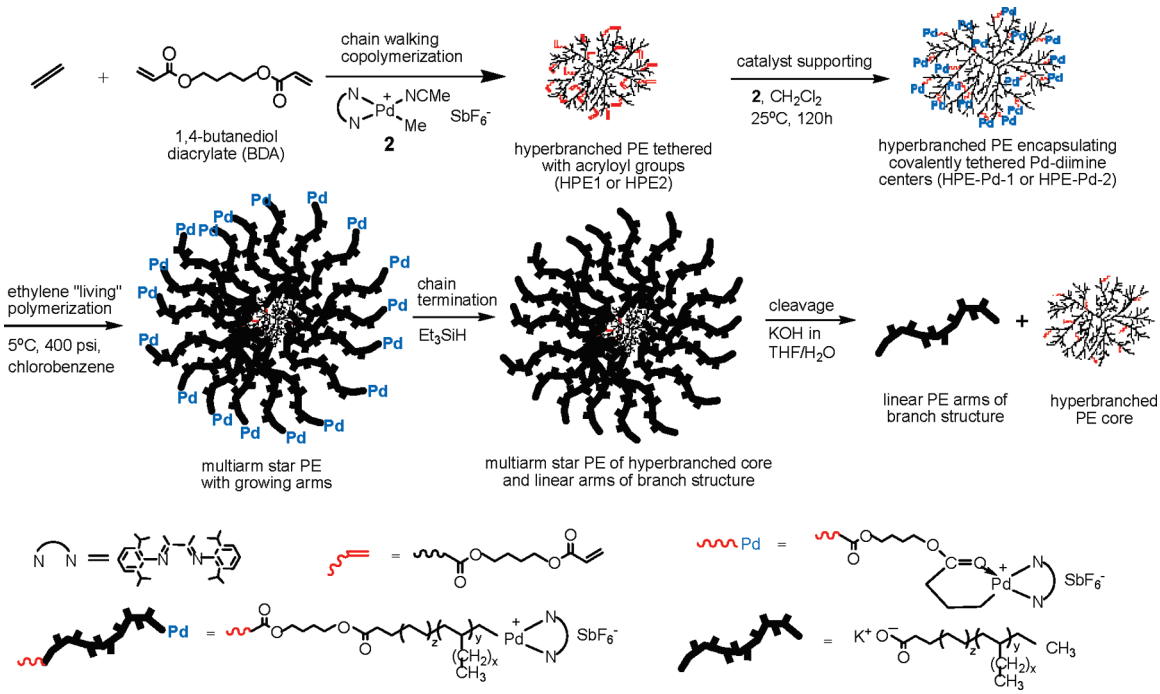

BDA feed concentrations, which inhibits/suppresses cross-linking reactions. With the chain walking mechanism of the catalyst, this nonliving copolymerization step yields hyperbranched polyethylenes containing pendant acryloyl groups with contents tunable by changing BDA feed concentration.[15]

In the second step, Pd−diimine catalysts are covalently tethered onto the hyperbranched polyethylene bearing the pendant acryloyl groups, by reacting with catalyst **2**, to render hyperbranched polyethylenes encapsulating covalently immobilized Pd−diimine ester chelate catalytic centers (or multinuclear hyperbranched Pd−diimine catalysts). This catalyst immobilization utilizes the characteristic reaction between catalyst **2** and the pendant acryloyl groups on the hyperbranched polymers, which are the specific catalyst anchoring sites herein, to form the ester chelate structure. In the reaction, the acryloyl double bond is inserted into the Pd-Me bond of **2** via 2,1-insertion, followed with subsequent rearrangement to give rise to a six-membered cyclic ester chelate structure.[22] This reaction chemistry has been used to synthesize trinuclear catalyst **1**,[13] functionalized Pd−diimine chelate catalysts,[17] and silica-supported Pd chelate catalysts[18] in our previous works. Herein, it renders cationic Pd−diimine chelate centers tethered/supported onto the hyperbranched polyethylene through the ester linkages. The hyperbranched polymer thus serves as the homogeneous support for the Pd−diimine catalysts. Under slight excess of catalyst **2**, all the pendant acryloyl groups in the hyperbranched polyethylene can potentially be converted into active Pd chelate centers. The average number of covalently immobilized Pd sites per chain in the Pd-encapsulating hyperbranched polyethylene is thus determined by the average number of acryloyl groups in the hyperbranched polyethylene synthesized in the first step.

In the subsequent third step of the procedure, the homogeneous hyperbranched polyethylene encapsulating the tethered Pd chelate catalysts is used to catalyze ethylene multifunctional "living" polymerization at a prescribed condition (ethylene pressure of 400 psi and 5 °C) for "core-first" synthesis of multiarm star polyethylenes. The Pd−diimine ester chelate catalysts have been well demonstrated to initiate and catalyze ethylene "living" polymerization at this condition to render narrow-distributed chains grown from the Pd-CH_2 initiating site in the 6-membered chelate structure.[13,17,18,24] This polymerization chemistry has previously enabled the synthesis of three-arm star polyethylenes[13] and end-functionalized telechelic polyethylenes,[17] as well as surface-initiated ethylene "living" polymerization for covalent surface grafting of polyethylene chains on silica nanoparticles.[18] With the homogeneous hyperbranched-polyethylene-supported Pd catalysts herein, this polymerization chemistry ought to lead to multiarm star polymers having multiple growing polyethylene chains with their starting ends joined at the hyperbranched core through the ester linkages. Given the "living" nature of this step, a control of the arm length in the star polymers can be achieved by tuning polymerization time. Moreover, the control of the average arm number is also expected by changing BDA feed concentration and other polymerization conditions in the first step, which determines the average number of acryloyl groups per polymer chain and subsequently the average number of the Pd catalytic centers immobilized on the hyperbranched core. This synthesis strategy should thus enable the synthesis of well-defined star polymers with controllable arm length and tunable average arm number.

Synthesis of Hyperbranched Polyethylenes Encapsulating Covalently Tethered Pd−Diimine Catalysts. With the first copolymerization step being well demonstrated, we directly employed herein two acryloyl-containing hyperbranched polyethylenes (HPE1 and HPE2), which were synthesized in our earlier work[15] by chain walking copolymerization of ethylene with BDA at elevated concentrations, to prepare two hyperbranched polyethylenes encapsulating covalently tethered Pd−diimine catalysts. Please find in the Experimental Section the polymerization conditions for the synthesis of these two polymers. Table 1 summarizes the structural information and molecular weight data of the two hyperbranched polymers. As confirmed in our earlier paper,[15]

Table 1. Structural and Molecular Weight Information of the Hyperbranched Polyethylenes (HPE1 and HPE2) Containing Pendant Acryloyl Groups

hyperbranched polyethylenes	total BDA content[a] (mol %)	acryloyl content[a] (mol %)	average number of acryloyl groups per chain[b]	$M_{w,LS}$[c] (kg/mol)	$M_{n,LS}$[c] (kg/mol)	PDI[c]	$[\eta]_w$[c] (mL/g)	branch. density[d] (per 1000 C)
HPE1	2.2	1.9	23	50	38	1.3	15	92
HPE2	1.5	1.3	32	136	74	1.8	20	105

[a] Determined with ^{1}H NMR spectroscopy in our earlier work.[15] [b] Calculated with the use of acryloyl content and $M_{n,LS}$ data. [c] Weight-average molecular weight ($M_{w,LS}$), number-average molecular weight ($M_{n,LS}$), and polydispersity index (PDI) were determined with the light scattering detector of the triple-detection GPC. Weight-average intrinsic viscosity ($[\eta]_w$) was determined with viscosity detector of the triple-detection GPC. [d] Total branching density in the ethylene sequences determined with ^{1}H NMR spectroscopy in our earlier work.[15]

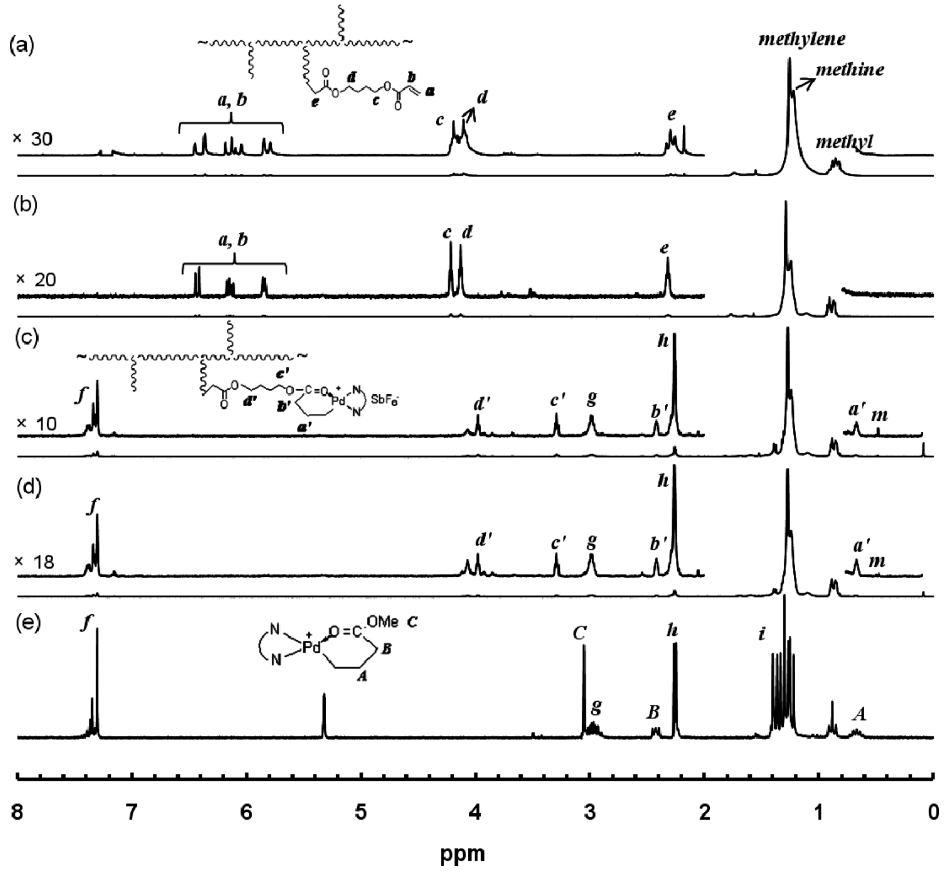

Figure 1. ^{1}H NMR spectra of (a) HPE1, (b) HPE2, (c) HPE-Pd-1, (d) HPE-Pd-2, and (e) the model mononuclear Pd−diimine chelate catalyst (**3**).

BDA was incorporated predominantly in them as pendant acryloyl groups with negligible inter- and/or intramolecular cross-linking. From ^{1}H NMR characterization (spectra shown in Figure 1, parts a and b), the two polymers have a BDA molar content of 2.2 and 1.5 mol %, respectively, and an acryloyl content of 1.9 and 1.3 mol %, respectively, which correspond to a selectivity of 86% for BDA monoinsertion in both polymers. Owing to the nonliving nature of this copolymerization step, both polymers show slight broad molecular weight distribution with a polydispersity index (PDI) of 1.3 and 1.8, respectively. Given the statistical distribution of the pendant acryloyl groups within each chain, this polydispersity in molecular weight suggests a distribution of the number of acryloyl groups per hyperbranched chain. With the use of absolute number-average molecular weight (M_n) determined with the light scattering detector in triple-detection GPC, the average number of acryloyl groups per chain is calculated to be 23 and 32 in HPE1 and HPE2, respectively. With the different average numbers of the tethered acryloyl groups per chain, these two polymers are expected to give rise to, in the subsequent steps, hyperbranched polyethylenes containing different average numbers of Pd sites and star polyethylenes having different average arm numbers. The hyperbranched chain topology of these two polymers has been verified in our earlier work on the basis of their low intrinsic viscosity and Newtonian flow behavior with low melt viscosity.[15]

Used as homogeneous supports with specific anchoring sites, HPE1 and HPE2 were reacted with catalyst **2** in CH_2Cl_2 for 5 days at room temperature to render the Pd-encapsulating hyperbranched polymers (HPE-Pd-1 and HPE-Pd-2, respectively). Relative to the number of pendant acryloyl groups, a slight excess amount of catalyst **2** (1.4 and 1.1 equiv, respectively) was applied in the reaction in an attempt to achieve near complete consumption of the acryloyl groups and maximum catalyst immobilization. During the course of the reaction, no gelation was observed. Because of the large hyperbranched structure of the two homogeneous polymer supports, the two resulting supported catalysts, HPE-Pd-1 and HPE-Pd-2, show good solubility in low-polarity diethyl ether or pentane while catalyst **2** is nearly insoluble in the two solvents. This distinctive solubility

Table 2. Ethylene "Living" Polymerization with HPE-Pd-1 at 400 psi and 5 °C[a]

			GPC−LS−VIS characterizations of as-produced multiarm star polymers[c]										
polymer sample	time (h)	polymer productivity[b] (g/h)	mass fraction	$M_{n,LS}$ (kg/mol)	$M_{w,LS}$ (kg/mol)	PDI	$f_{n,arm}$[d]	$[\eta]_w$ (mL/g)	$R_{g,w}$ (nm)	$R_{h,w}$ (nm)	ρ[e]	α[e]	α_s[e]
SPE1-1	1	0.82	0.90	205	411	2.0	21	32	12	12	1.0	0.20	0.37
SPE1-2	2	0.80	0.83	400	746	1.9	22	44	17	16	1.1	0.073	0.37
SPE1-3	3	0.81	0.79	542	947	1.8	21	52	19	18	1.0	0.019	0.36
SPE1-4	4	0.78	0.77	699	1234	1.8	21	62	20	21	0.95	−0.013	0.35
SPE1-5	5	0.87	0.69	762	1267	1.7	19	70	22	22	1.0	−0.029	0.31
SPE1-6	6	0.87	0.72	1192	1920	1.6	24	78	27	27	1.0	−0.074	0.23

[a] Other polymerization conditions: HPE-Pd-1 amount, 0.18 g; solvent, chlorobenzene (150 mL) and dichloromethane (10 mL). [b] Polymer productivity defined as (mass of polymer obtained)/(polymerization time). [c] Triple-detection GPC characterization results of the as-produced star polymers within the higher-molecular-weight peaks in the GPC elution traces. The lower-molecular-weight peaks were excluded in the calculation. The M_n, M_w, PDI, and weight-average gyration radius ($R_{g,w}$) data were determined with the light scattering detector, and weight-average intrinsic viscosity ($[\eta]_w$) and weight-average hydrodynamic radius ($R_{h,w}$) were determined with the viscosity detector. [d] The number-average arm number ($f_{n,arm}$) is calculated as (M_n of the star polymer − M_n of the hyperbranched core)/(M_n of arm). The M_n of the arm is calculated from the linear fitting equation shown in Figure 4 for the linear polymers synthesized with catalyst **3**. [e] ρ factor is defined as $\rho = R_{g,w}/R_{h,w}$. α is the Mark−Houwink exponent. α_s is the exponent for the dependence of R_g on molecular weight.

difference facilitates the convenient removal of the majority of the unreacted **2** in the products through an dissolution-filtration procedure (see Experimental Section).

To confirm the successful covalent catalyst immobilization, both HPE-Pd-1 and HPE-Pd-2 were subsequently characterized with ^{1}H NMR spectroscopy. The homogeneous nature of both supported catalysts allows the elucidation of the exact structure of the immobilized Pd catalysts with NMR. Parts c and d of Figure 1 show the ^{1}H NMR spectra of HPE-Pd-1 and HPE-Pd-2, respectively. Like the spectra of both HPE1 and HPE2, the major peaks in the spectra of HPE-Pd-1 and HPE-Pd-2 are the methyl, methylene, and methine protons of the ethylene sequences of the hyperbranched polyethylene supports. Compared to the spectra of HPE1 and HPE2, the resonance peaks corresponding to the acryloyl double bonds (peaks *a*, *b* in Figure 1a,b) are absent in the spectra of HPE-Pd-1 and HPE-Pd-2, suggesting the complete consumption of the acryloyl double bonds. Meanwhile, new peaks (peaks *a*′−*d*′, *f*−*h*) assignable to the immobilized Pd chelate catalysts appear. Among them, peaks *f* (7.25−7.45 ppm), *g* (3.00 ppm), and *h* (2.26 ppm) are attributed to the protons on the diimine ligand, and peaks *a*′ (0.67 ppm) and *b*′ (2.42 ppm) correspond, respectively, to the protons of two CH_2 groups on the six-membered catalyst chelate structure, Pd$CH_2CH_2CH_2$C(O).[17] Meanwhile, peak *c*′ (3.30 ppm) is assigned to the methylene protons most adjacent to the ester chelate structure and peak *d*′ (3.98 ppm) should be the protons of the CH_2 group next to the other ester functionality. The assignment of these new peaks is in good agreement with those of the model mononuclear Pd−diimine chelate catalyst (**3** in Scheme 1) shown in Figure 1e and other well-defined Pd−diimine chelate catalysts we synthesized earlier.[13,17] The appearance of these new peaks confirms the successful covalent tethering of Pd−diimine chelate centers.

On the basis of peak integration, the average number of covalently tethered Pd chelate centers is estimated to be about 76% and 70% of the number of acryloyl groups in HPE1 and HPE2, respectively. Therefore, the average number of tethered Pd chelate centers is about 17 and 23 per polymer chain in HPE-Pd-1 and HPE-Pd-2, respectively. The incomplete conversion of pendant acryloyl groups to Pd chelate catalysts may possibly result from catalyst decomposition after immobilization and/or other side reaction involving the acryloyl double bonds, such as a low level of radical incurred inter- or intracross-linking, during the catalyst immobilization. In addition to the covalently tethered Pd chelate centers, a small amount of residual nonreacted **2** is also found to exist in both HPE-Pd-1 and HPE-Pd-2 despite several cycles of purification. In Figure 1, parts c and d, peak m (0.48 ppm) and another one at 1.81 ppm are observed and they are attributed to methyl protons of PdCH_3 and PdNCCH_3, respectively, in **2**.[17b] On the basis of peak integration, the amount of residual **2** is somehow low, about 6% and 3% of the covalently tethered Pd chelate centers in HPE-Pd-1 and HPE-Pd-2, respectively. Such residual **2** is probably physically encapsulated within the hyperbranched polymers and is thus difficult to achieve a complete removal during the purification procedure. As will be demonstrated below, such mononuclear residual **2** can also catalyze ethylene "living" polymerization in the subsequent third step, generating a low-molecular-weight polymer fraction compared to the high-molecular-weight multiarm star polymers. Because of the covalent encapsulation of organometallic Pd−diimine species, both HPE-Pd-1 and HPE-Pd-2 appear as brown nonsticky elastic solid at room temperature, which differs significantly from the highly sticky low-viscosity oil-like HPE1 and HPE2.[15]

Synthesis of Multiarm Star Polyethylenes by Ethylene Multifunctional "Living" Polymerization with HPE-Pd-1 and HPE-Pd-2 at 400 psi and 5 °C. Ethylene "living" polymerizations were subsequently carried out with HPE-Pd-1 and HPE-Pd-2 in chlorobenzene, respectively, for "core-first" synthesis multiarm star polyethylenes. A typical polymerization condition, ethylene pressure of 400 psi and 5 °C, was used herein as cationic Pd−diimine catalysts have been well demonstrated to successfully initiate and catalyze ethylene "living" polymerization at this condition.[13,17,18,24] Both polymerizations were undertaken for a total polymerization time of 6 h, and polymerization solutions were sampled every hour in order to monitor polymer molecular weight development as a function of time. The sampled solutions were all quenched with Et_3SiH, rendering saturated polymer terminal ends.[24] After polymer purification by removal of Pd catalyst residue, we obtained two sets of as-produced polymers, the SPE1 set (polymers SPE1-1 to SPE1-6 with the last digit indicating polymerization hours) obtained with HPE-Pd-1 and SPE2 set (polymers SPE2-1 to SPE2-6, also with the last digit indicating polymerization hours) obtained with HPE-Pd-2. These polymers were characterized with a triple-detection GPC incorporating online differential refractive index (DRI), three-angle light scattering (LS), and viscosity detectors. THF was used as the GPC mobile phase since all polymers dissolve well in it even at room temperature. Tables 2 and 3 summarize the polymerization results and the data obtained from GPC characterization.

Table 3. Ethylene "Living" Polymerization with HPE-Pd-2 at 400 psi and 5 °C[a]

			GPC−LS−VIS characterizations of as-produced multiarm star polymers[c]										
polymer sample	time (h)	polymer productivity[b] (g/h)	mass fraction	$M_{n,LS}$ (kg/mol)	$M_{w,LS}$ (kg/mol)	PDI	$f_{n,arm}$[d]	$[\eta]_w$ (mL/g)	$R_{g,w}$ (nm)	$R_{h,w}$ (nm)	ρ[e]	α[e]	α_s[e]
SPE2-1	1	2.56	0.85	292	675	2.3	27	36	16	14	1.1	0.18	0.40
SPE2-2	2	1.47	0.87	572	1146	2.0	31	48	19	19	1.0	0.084	0.36
SPE2-3	3	2.24	0.85	760	1344	1.8	29	55	22	21	1.0	0.035	0.33
SPE2-4	4	1.56	0.87	969	1792	1.8	28	64	23	24	0.96	−0.006	0.29
SPE2-5	5	1.28	0.82	1130	2019	1.8	27	71	25	26	0.96	−0.027	0.28
SPE2-6	6	1.43	0.81	1379	2379	1.7	27	80	28	29	0.96	−0.053	0.25

[a] Other polymerization conditions: HPE-Pd-2 amount, 0.84 g; solvent, chlorobenzene (300 mL) and dichloromethane (20 mL). [b] Polymer productivity defined as (mass of polymer obtained)/(polymerization time). [c] Triple-detection GPC characterization results of the as-produced star polymers within the higher-molecular-weight peaks in the GPC elution traces. The lower-molecular-weight peaks were excluded in the calculation. The M_n, M_w, PDI, and $R_{g,w}$ data were determined with the light scattering detector, and $[\eta]_w$ and $R_{h,w}$ were determined with the viscosity detector. [d] The number-average arm number ($f_{n,arm}$) is calculated as (M_n of the star polymer − M_n of the hyperbranched core)/(M_n of arm). The M_n of the arm is calculated from the linear fitting equation shown in Figure 4 for the linear polymers synthesized with catalyst **3**. [e] ρ factor is defined as $\rho = R_{g,w}/R_{h,w}$. α is the Mark−Houwink exponent. α_s is the exponent for the dependence of R_g on molecular weight.

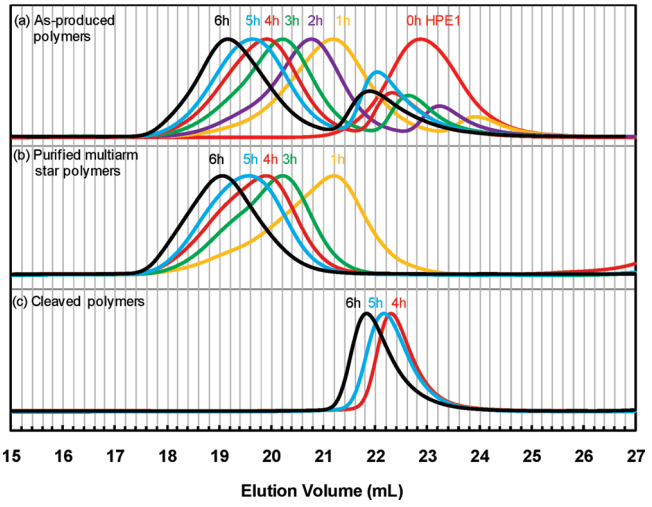

Figure 2. GPC elution traces (from DRI detector) of (a) the SPE1 set of as-produced polymers obtained at different polymerization time in ethylene "living" polymerization with HPE-Pd-1 at 400 psi and 5 °C, (b) their purified star polymers obtained by GPC fractionation with low-molecular-weight linear polymer peak removed, and (c) the cleaved polymers obtained by alkaline hydrolysis of the corresponding as-produced SPE1 polymers.

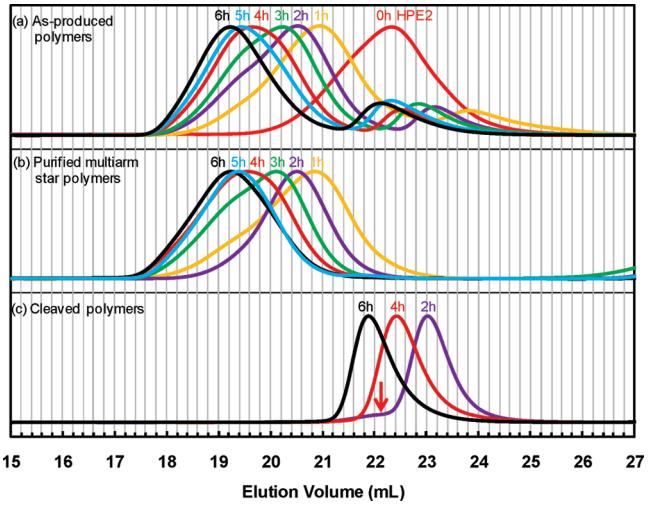

Figure 3. GPC elution traces (from DRI detector) of (a) the SPE2 set of as-produced polymers obtained at different polymerization time in ethylene "living" polymerization with HPE-Pd-2 at 400 psi and 5 °C, (b) their purified star polymers obtained by GPC fractionation with low-molecular-weight linear polymer peak removed, and (c) the cleaved polymers obtained by alkaline hydrolysis of the corresponding as-produced SPE2 polymers.

Figures 2a and 3a show, respectively, the GPC elution traces of the two sets of as-produced polymers obtained from the DRI detector (i.e., concentration detector) in triple-detection GPC measurements. Bimodal GPC traces with a dominant high-molecular-weight peak and a minor low-molecular-weight peak are observed for all the as-produced polymers in both sets. In each polymer, the two peaks are generally well separated from each other with little peak overlapping, indicating the significant difference in polymer molecular weight between the two peaks. With the increase of polymerization time, both peaks move consistently toward to the left (i.e., reduced elution volume) in both sets of polymers, indicating the continuous increase of polymer molecular weight with time for both peaks. In each polymer, the high-molecular-weight peak has a similar peak shape compared to the corresponding acryloyl-containing hyperbranched polyethylene (HPE1 and HPE2, respectively). These high-molecular-weight peaks should thus correspond to the multiarm star polymers resulting from the multinuclear hyperbranched catalysts, whose arms grow incrementally longer from the hyperbranched core with the increase of polymerization time.

The low-molecular-weight peak in each GPC curve should correspond to polymers produced from the mononuclear catalyst **2** residues physically present within HPE-Pd-1 and HPE-Pd-2 as shown above, and/or Pd catalytic centers leached into the solution after experiencing undesired chain transfer side reactions. The acetonitrile complex **2** has been well demonstrated to catalyze, like the ester chelate catalysts, ethylene "living" polymerization at the given condition.[24] Meanwhile, the occurrence of chain transfer reactions in Pd−diimine catalyzed ethylene "living" polymerization at 400 psi and 5 °C has been observed, though at low levels, in our earlier studies.[13,17] Herein, the occurrence of the side reactions will lead to the permanent termination of the growth of some arms and release of the associated Pd active sites bound on the growing star polymers into the solution to become mononuclear Pd centers capable of initiating new "living" chains. These two types of mononuclear Pd centers should have the same cationic active site structure as those bound on the growing star polymers and consequently, they should have the equal capability of initiating and catalyzing "living" chain growth at the same polymerization condition. The resulting low-molecular-weight polymers from these mononuclear catalysts should thus have similar chain microstructure and average molecular weights as the arms in the high-molecular-weight star polymers produced from bound

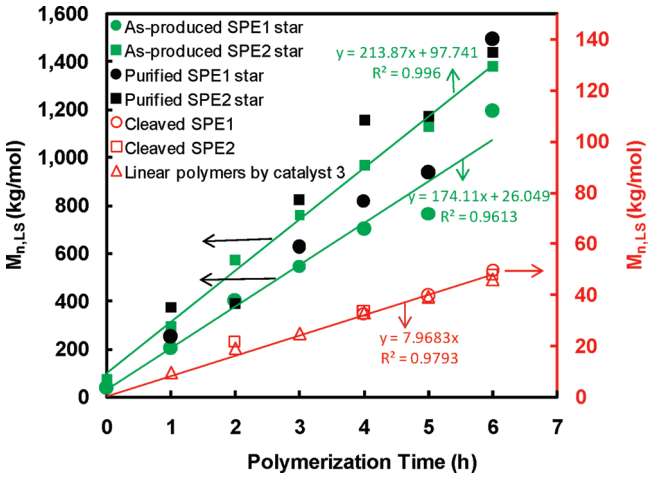

Figure 4. Plot of $M_{n,LS}$ determined with LS detector versus polymerization time for both SPE1 and SPE2 sets of as-produced star polymers (with low-molecular-weight linear polymer peaks excluded), their purified star polymers and cleaved polymers, and the polymers by catalyst **3** at 400 psi and 5 °C. The linear fitting curves and equations are generated for both sets of as-produced star polymers and the polymers by catalyst **3**.

catalysts at the same polymerization time. Comparing each pair of parallel polymers obtained after the same polymerization time in the two sets (SPE1 and SPE2), it can be found that their low-molecular-weight peaks indeed have nearly identical elution volumes (i.e., similar molecular weights) despite that they were produced in two different polymerizations. This verifies the assignments of the low-molecular-weight peaks to polymers produced with mononuclear catalyst species. Given the high ethylene pressure of 400 psi and low temperature of 5 °C employed herein, the arms and these lower-molecular-weight polymers should have a linear topology but with short branch structures resulting from catalyst chain walking on the basis of our earlier studies.[19]

By performing peak integration on the GPC elution traces obtained from the DRI detector, the mass fractions for the multiarm star polymers in the high-molecular-weight peaks are determined and are listed in Tables 2 and 3. With the increase of polymerization time, a slight but consistent decrease in mass fraction of the star polymers is observed in both sets of as-produced polymers (from 0.90 in SPE1-1 to 0.72 in SPE1-6, and from 0.85 in SPE2-1 to 0.81 in SPE2-6), with the corresponding increase in the mass fraction for the low-molecular-weight linear polymers. This confirms the presence of undesired chain transfer reactions and/or active site deactivation, which become increasingly obvious with the increase of polymerization time.[13] Such side reactions render dead arms, which cannot grow further. For all the as-produced polymers, their GPC elution traces from the viscosity detector are also clearly bimodal with the presence of both high-molecular-weight and low-molecular-weight peaks. The GPC traces collected from the LS detector, however, are nearly monomodal, with a negligibly weak low-molecular-weight peak situated on the right tail of the high-molecular-weight star polymer peak. This is due to the much reduced molecular weight of the linear polymers as the light scattering signals show a dependence on both polymer molecular weight and concentration.[25]

With the three-angle LS detector, the absolute molecular weights and molecular weight distribution of the star polymers in the high-molecular-weight peaks were determined for both sets of as-produced polymers. In the calculation, the linear polymers in the low-molecular-weight GPC peaks were excluded. This exclusion should not affect the molecular weight data of the star polymers due to their well-separated GPC peaks with negligible peak overlapping as shown above. For the low-molecular-weight linear polymers, their molecular weight information cannot be accurately determined with the LS detector due to their very weak light scattering intensity and significant peak broadening resulting from the tail of the high-molecular-weight peak. The molecular weight data are listed in Tables 2 and 3, respectively. In Figure 4, the dependencies of M_n on polymerization time for both sets of as-produced star polymers are shown. Compared to the corresponding hyperbranched core (HPE1 or HPE2), the star polymers in both sets show increasingly higher molecular weights with the increase of polymerization time. In the SPE1 set, SPE1-1 star polymer has M_n of 205 kg/mol and SPE1-6 star polymer has M_n of 1,192 kg/mol, which are much higher compared to the M_n value of 38 kg/mol for the hyperbranched core HPE1. In the SPE2 set, SPE2-1 star polymer has M_n of 292 kg/mol and SPE2-6 star polymer has M_n of 1,379 kg/mol in contrast to the M_n value of 74 kg/mol for the core HPE2. This consistent enhancement in molecular weight confirms the continuous arm growth in the multiarm star polymers during the polymerization. On the basis of their molecular weight data, the mass fraction of the hyperbranched core in the star polymers should thus be low.

From Figure 4, the M_n value increases almost linearly with the increase of polymerization time for both sets of as-produced star polymers, which is the characteristic of "living" polymerization.[13,17,24] This linear increase of molecular weight provides the evidence supporting that the two polymerizations with both multinuclear hyperbranched catalysts are truly multifunctional "living" polymerization wherein the tethered Pd−diimine catalysts initiate and catalyze the simultaneous "living" arm growth in multiple directions. Given the identical polymerization condition employed herein, the arm length should be similar in the star polymers obtained at a same polymerization time in both sets. Compared to the corresponding star polymers obtained at a same polymerization time in SPE1 set, the star polymers in the SPE2 set generally have higher average molecular weights and a stronger dependence of M_n on polymerization time (from the slopes of the linear fitting lines in Figure 4). This indicates the higher average number of arms in the SPE2 set of star polymers, which is consistent with the higher average number of Pd sites in HPE-Pd-2 shown above. Compared to the hyperbranched core, the multiarm star polymers generally have higher PDI values (1.6−2.0 for the SPE1 set; 1.7−2.3 for the SPE2 set), which, however, is reduced slightly with an increase of polymerization time. This polydispersity in molecular weight reflects the distribution of arm number per chain in the star polymers, which should originate from the distribution of the number of tethered Pd sites per chain in HPE-Pd-1 and HPE-Pd-2. Meanwhile, the distributions in arm length and the hyperbranched core may also contribute to the molecular weight distribution of the star polymers.

The as-produced polymers were characterized with ^{1}H NMR spectroscopy. Representatively, Figure 5 shows and compares the ^{1}H NMR spectra of three selected SPE2 polymers, SPE2-2, SPE2-4, and SPE2-6. Besides the dominant peaks from the ethylene sequences, the resonance peaks (*j* at 4.10 ppm and *k* at 2.30 ppm in Figure 5) resulting from the diester linkages ($CH_2CO(O)CH_2(CH_2)_2CH_2O(O)CCH_2$) can be clearly seen.[13] These diester linkages, evolving from the originally incorporated BDA units in the first step of the synthesis procedure, bind covalently the polymer arms to the hyperbranched core. With the increase of polymerization time, the relative concentration of these linkages in the

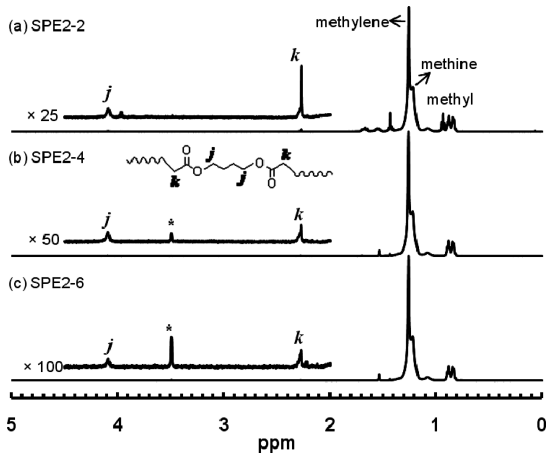

Figure 5. ^{1}H NMR spectra of the representative as-produced polymers in the SPE2 set: (a) SPE2-2; (b) SPE2-4; (c) SPE2-6.

polymers is reduced (from Figure 5) due to the increase of the arm length. The branch density of the ethylene sequences was calculated by integration of the methyl, methylene, and methine peaks in the ^{1}H NMR spectra, and was determined to be about 86 per 1000 carbons for all three polymers. As the mass percentage of the hyperbranched core should be low in the as-produced polymers (the highest among the three is about 11% in SPE2-2), this branching density should reflect primarily the chain microstructure of the polyethylenes produced in the "living" polymerization step, i.e., the polymer arms in the star polymers and the linear low-molecular-weight polymers by mononuclear catalysts. This branching density data is very close to those of polyethylenes produced by several mononuclear Pd−diimine catalysts at the same condition in our previous works,[13,17] which have linear topology but contain short branching structures.

Cleavage of As-Produced Polymers. To determine the arm length and average arm number in the multiarm star polymers, cleavage experiments were conducted on some as-produced polymers (SPE1-4 to SPE1-6, SPE2-2, SPE2-4, and SPE2-6) available in larger amounts in both sets by alkaline hydrolysis of the diester linkages to cleave off the arms from the hyperbranched core.[13] The cleaved polymers were characterized with triple-detection GPC. Figure 2c and Figure 3c show, respectively, the GPC elution traces (from DRI detector) of the cleaved polymers in the two sets. Each cleaved polymer should be a polymer mixture, including the cleaved arms, the hyperbranched core, and linear low-molecular-weight polymer present originally in the as-produced polymer. Among them, the mass percentage of the hyperbranched core should be very low (the highest one among all the cleaved polymers is 11% for SPE2-2), and the cleaved arms and the linear polymers by mononuclear catalysts should have nearly equal molecular weight following the above discussion. From Figures 2c and 3c, all the cleaved polymers, except the one for SPE2-2, show a single narrow GPC elution peak with no additional peaks attributable to the corresponding hyperbranched core or low-molecular-weight linear polymers, thus confirming our hypothesis. With exception, the cleaved polymer for SPE2-2 shows a weak GPC tail at the high-molecular-weight end (indicated with an arrow in Figure 3c), which should correspond to the hyperbranched core (HPE2) on the basis of its elution volume range. Among these cleaved polymers, the mass fraction for the hyperbranched core should be highest in SPE2-2 given the shortest arm length in this polymer resulting from the shortest polymerization time, which renders its visibility in the GPC elution trace of the cleaved polymer.

For each cleaved polymer, the GPC elution peak has much higher elution volume (i.e., much lower molecular weight) compared to the high-molecular-weight peak in its original as-produced polymer. This confirms the construction of the star polymers with the arms. Moreover, the elution volume of each cleaved polymer is almost identical to the corresponding low-molecular-weight peak, resulting from the mononuclear catalyst species, in the biomodal GPC trace of its as-produced polymer. This further supports that the arms and the linear low-molecular-weight polymers have nearly equal molecular weight. The absolute molecular weight data of the cleaved polymers were also determined with the LS detector of the triple-detection GPC. The results are summarized in Table 4, and the dependency of M_n on polymerization time on these cleaved polymers is also shown in Figure 4. In Figure 4, we have also included the molecular weight data for the linear polymers produced via ethylene "living" polymerization using the model mononuclear catalyst **3** at the same condition (400 psi and 5 °C), which show a linear dependency of M_n on polymerization time with narrow PDI (about 1.0). Obtained in our earlier study,[13] these data are included herein for the purpose of comparison. As the arms and the linear polymers of similar molecular weights are the dominant components in each cleaved polymer, the molecular weight data of the cleaved polymers measured herein should be close to the true ones of the polymer arms. It can be found from Figure 4 that the cleaved polymers of both sets of as-produced polymers have nearly identical M_n values as the narrow-distributed polymers produced with catalyst **3** at the same polymerization time, with only very slight differences resulting possibly from the presence of the hyperbranched core. This indicates that each Pd active site tethered on the hyperbranched core or growing star polymers behaves identically as the homogeneous mononuclear Pd catalysts. Moreover, the nearly linear increase of M_n value with time and their low PDI (about 1.0 shown in Table 4) further confirm that the arm growth is a "living" process though with a low level of side reactions as discussed above. The molecular weight of the corresponding linear polymers synthesized by catalyst **3** at the same polymerization time can thus be used as the arm length in the star polymers.

The number-average arm number ($f_{n,arm}$) of the star polymers in the as-produced polymers was thus calculated by using the molecular weights of the polymers produced with catalyst **3** as the corresponding arm lengths. The data are also listed in Tables 2 and 3. The average arm number is typically about 21 and 28 arms per chain, respectively, for the SPE1 and SPE2 sets of star polymers. In both sets, only small variations are observed in the average arm number with the increase of polymerization time, consistent with their "living" polymerization behavior. Compared to the SPE1 set, the higher average arm number with the SPE2 set should be ascribed to the higher average number of tethered Pd sites in HPE-Pd-2 and, originally, the higher average number of acryloyl groups in HPE2. These average arm numbers are, however, slightly higher compared to the average number of Pd sites per chain (17 and 23 in HPE-Pd-1 and HPE-Pd-2) determined earlier. This may result from unavoidable characterization/measurement errors and/or the potential presence of radical induced intermolecular cross-linking reactions in the second step for catalyst immobilization, which renders slightly higher Pd loading numbers per hyperbranched chain than calculated. Despite this, the results confirm solidly that a control of the average acryloyl number per chain in the hyperbranched polymer in the first synthesis step renders the eventual tuning of average arm number in the multiarm star polymers.

Table 4. Triple-Detection GPC Characterization Results of Purified Multiarm Star Polymers and Cleaved Polymers from both SPE1 and SPE2 Sets of As-Produced Polymers[a]

	purified multiarm star polymers										cleaved polymers			
polymer sample	$M_{n,LS}$ (kg/mol)	$M_{w,LS}$ (kg/mol)	PDI	$f_{n,arm}$[b]	$[\eta]_w$ (mL/g)	$R_{g,w}$ (nm)	$R_{h,w}$ (nm)	ρ[c]	α[c]	α_s[c]	$M_{n,LS}$ (kg/mol)	$M_{w,LS}$ (kg/mol)	PDI	$[\eta]_w$ (mL/g)
SPE1-1	249	682	2.7	26	36	17	14	1.2	0.24	0.37				
SPE1-3	624	1150	1.8	24	54	20	20	1.0	0.034	0.37				
SPE1-4	817	1486	1.8	24	63	22	23	0.96	0.024	0.37	32.6	33.2	1.0	33
SPE1-5	938	1632	1.7	23	72	23	25	0.92	−0.014	0.34	39.7	40.2	1.0	37
SPE1-6	1496	2591	1.7	30	81	29	30	0.97	−0.033	0.30	49.3	50.3	1.0	42
SPE2-1	371	870	2.3	37	39	20	16	1.2	0.21	0.41				
SPE2-2	389	586	1.5	20	46	15	15	1.0	0.073	0.44	21.6	22.4	1.0	23
SPE2-3	822	1614	2.0	31	57	24	22	1.1	0.078	0.37				
SPE2-4	1155	2265	2.0	34	67	31	27	1.1	0.059	0.42	33.7	34.6	1.0	32
SPE2-5	1169	2029	1.7	27	75	27	28	0.96	0.029	0.30				
SPE2-6	1436	2573	1.8	28	81	32	29	1.1	−0.023	0.30	47.9	48.8	1.0	42

[a] The M_n, M_w, PDI, and $R_{g,w}$ data were determined with the light scattering detector, and $[\eta]_w$ and $R_{h,w}$ data were determined with the viscosity detector. [b] The number-average arm number ($f_{n,arm}$) is calculated as (M_n of the star polymer − M_n of the hyperbranched core)/(M_n of arm). The M_n of the arm is calculated from the linear fitting equation shown in Figure 4 for the linear polymers synthesized with catalyst **3**. [c] ρ factor is defined as $\rho = R_{g,w}/R_{h,w}$. α is the Mark−Houwink exponent. α_s is the exponent for the dependence of R_g on molecular weight.

Purification of As-Produced Polymers. Purification of the two sets of as-produced polymers was carried out with a preparative GPC fractionation technique (see Experimental Section) to obtain the purified multiarm star polymers with the low-molecular-weight linear polymers removed. The large molecular weight difference between them enables successful and convenient polymer fractionation. With the GPC fractionation technique, about 85% of the star polymers in the high-molecular-weight peaks were obtained to render the respective purified star polymers. These purified star polymers were also characterized with triple-detection GPC. Their GPC elution traces are shown in Figures 2b and 3b, respectively. In general, the purified star polymers have very similar GPC peak shape and width as the corresponding high-molecular-weight peaks in the as-produced polymers. The peaks for low-molecular-weight linear polymers are absent, indicating the complete removal of the low-molecular-weight linear side products. The molecular weight data of the purified star polymers are listed in Table 4 and the dependency of their M_n on polymerization time is also constructed in Figure 4. Compared to the corresponding star polymers in the as-produced polymers, the purified star polymers generally show higher molecular weights due to the unavoidable loss of some lower-molecular-weight star polymer portions during polymer fractionation.

Dilute Solution Properties and Chain Conformation of Multiarm Star Polymers. The triple-detection GPC incorporating the LS and viscosity detectors also allows the efficient convenient determination of the dilute solution properties (in THF as a good solvent at 33 °C) of this novel range of multiarm core−shell structured star polymers synthesized herein, in addition to their absolute molecular weight show above. In particular, the gyration radius (R_g) of each polymer elution fraction is determined with the three-angle LS detector on the basis of the angular dependency of light scattering intensity, and the intrinsic viscosity ($[\eta]$) and hydrodynamic radius ($R_h = [3M[\eta]/10\pi N_a]^{1/3}$)[25] are simultaneously determined with the viscosity detector. By integration over the whole molecular weight distribution, average values of these properties can be obtained, such as weight-average intrinsic viscosity ($[\eta]_w$), weight-average gyration radius ($R_{g,w}$), and weight-average hydrodynamic radius ($R_{h,w}$). The data for these dilute solution properties are also summarized in Tables 2−4, respectively. These dilute solution properties enable us to examine the chain conformation of these novel star polymers.

Figure 6 shows the dependencies of intrinsic viscosity on polymer molecular weight (i.e., Mark−Houwink plot) for the polymers in the SPE1 set, including the as-produced star polymers, their purified star polymers and cleaved polymers, along with those of the hyperbranched core HPE1 and the polymers by model catalyst **3** for comparison. The Mark−Houwink exponent (α) is calculated from the slope of the intrinsic viscosity curve for each polymer in the plot. Generally, the as-produced star polymers and their corresponding purified star polymers show very similar intrinsic viscosity curves. With the increase of polymerization time (i.e., arm length), the viscosity curve is consistently raised, accompanied by a significant reduction in the slope (i.e., α value). With the as-produced star polymers as an example, the value of α is reduced continuously from a small positive number (0.20 for SPE1-1) to nearly zero (0.073 for SPE1-2 and 0.019 for SPE1-3) and to negative numbers (−0.013, −0.029, and −0.074 for SPE1-4 to SPE1-6, respectively) (see Table 2). The value of α is related to polymer chain conformation, typically with 0 for rigid spheres, 0.5 and 0.8 for flexible polymers in Θ solvents and good solvents, respectively, and 2 for rods.[25] Negative α values have also been found with spherical dendrimers of high generations[26,27] and some star polymers of high molecular weights.[28] Some

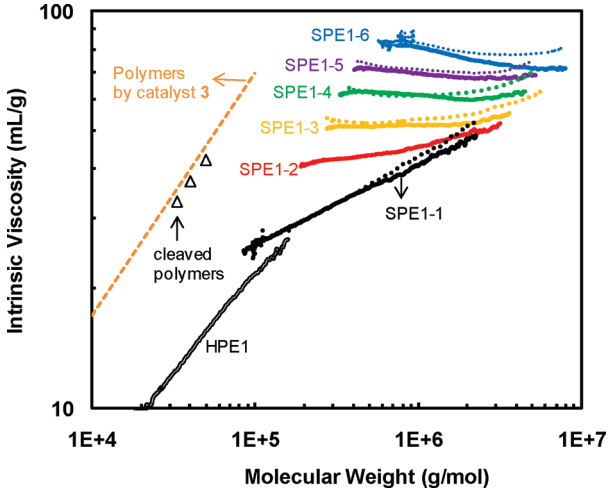

Figure 6. Mark−Houwink plot of the SPE1 set of polymers, including as-produced star polymers (in solid lines, with low-molecular-weight linear polymers excluded), purified star polymers (in dotted lines), cleaved polymers, and the hyperbranched polyethylene core (HPE1). The intrinsic viscosity curve obtained in our earlier study[13] for polymers synthesized by catalyst **3** at 400 psi and 5 °C is also included for comparison.

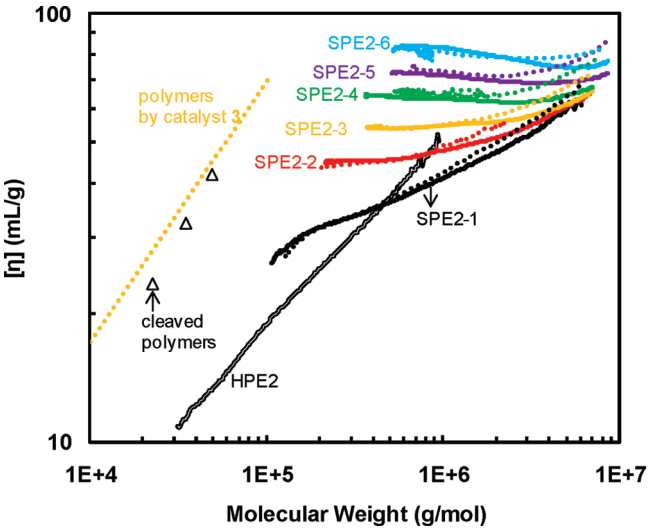

Figure 7. Mark−Houwink plot of the SPE2 set of polymers, including as-produced star polymers (in solid lines, with low-molecular-weight linear polymers excluded), purified star polymers (in dotted lines), cleaved polymers, and the hyperbranched polyethylene core (HPE2). The intrinsic viscosity curve obtained in our earlier study[13] for polymers synthesized by catalyst **3** at 400 psi and 5 °C is also included for comparison.

multiarm star polymers and hyperbranched polymers have also been demonstrated to behave as rigid spheres with zero α value, i.e., intrinsic viscosity does not change with molecular weight.[28−30] Herein, the reduction of the α value with the increase of polymerization time indicates that these multiarm star polymers evolve to behave like rigid spheres and, furthermore, spherical high-generation dendrimers with the continuous increase of the arm length.

In Figure 6, the viscosity values of the three cleaved SPE1 polymers are almost located on the intrinsic viscosity curve, $[\eta] = 0.0621\ M^{0.61}$ (mL/g), constructed in our earlier report for the linear polymers synthesized with model mononuclear catalyst **3** at the same condition.[13] Only very small deviations are noticed compared to the polymers by catalyst **3**, possibly resulting from the presence of the small fraction of the compact hyperbranched core in the cleaved polymers. This further confirms that the polymer arms have the same linear chain topology as the polymers produced with the mononuclear catalysts. Meanwhile, it is also evident from Figure 6 that the hyperbranched core HPE1 has much more compact chain topology compared to the linear arms given its much lower intrinsic viscosity curve. The intrinsic viscosity data of the star polymers are much lower compared to the linear polymers of an equal molecular weight. From Tables 2 and 4, the $[\eta]_w$ value for each star polymer (both as-produced and purified) is always about twice of that for the corresponding cleaved polymer (i.e., polymer arm) despite their very different molecular weights. This indicates that $[\eta]$ values of these star polymers of high average arm number are primarily determined by the arm length.[31]

Figure 7 shows the Mark−Houwink plot for the polymers in the SPE2 set. Very similar features discussed above are found with the polymers in this set. With the increase of arm length, the conformation of the star polymers quickly approaches to those of rigid spheres and high-generation dendrimers. Though this set of star polymers (both as-produced and purified) have a slightly higher average arm number compared to those in the SPE1 set, no significant difference in $[\eta]_w$ is found between any two parallel star polymers in the two sets produced at the same polymerization time (i.e., similar arm length). This further

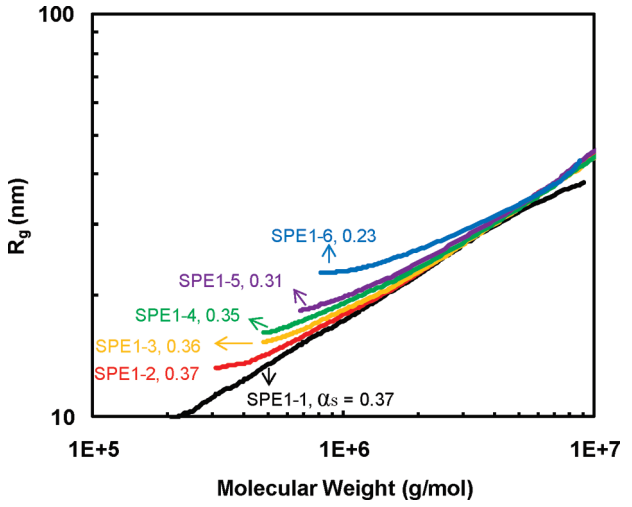

Figure 8. Gyration radius (R_g) versus polymer molecular weight for the SPE1 set of as-produced star polymers (with low-molecular-weight linear polymers excluded).

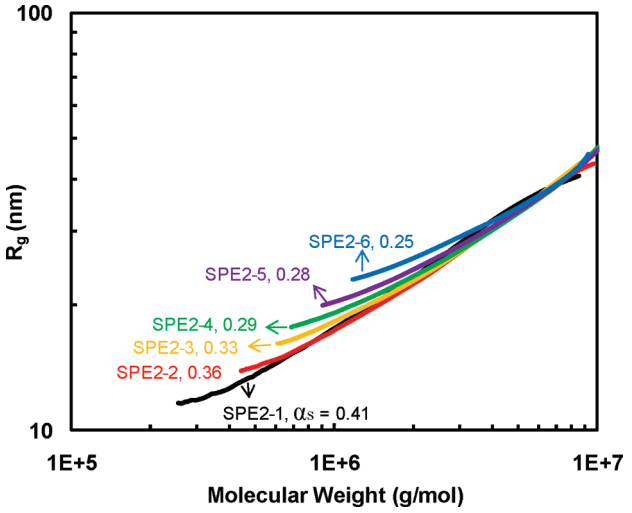

Figure 9. Gyration radius (R_g) versus polymer molecular weight for the SPE2 set of as-produced star polymers (with low-molecular-weight linear polymers excluded).

confirms that $[\eta]$ value is insensitive to arm numbers in these star polymers.[31]

Figures 8 and 9 show, respectively, the dependencies of R_g on molecular weight for the two sets of as-produced star polymers. Because of their low molecular weights, the R_g data for the cleaved polymers and the hyperbranched polymers (HPE1 and HPE2) could not be determined. Following the scaling law $R_g \propto M^{\alpha_s}$, the slope of the R_g curve in the plot gives the exponent α_s, which shows the dependency of R_g on molecular weight. Generally, α_s has a value of $^1/_3$ for rigid spheres of uniform density, 0.5 for flexible polymers in theta solvents, and 0.6 for flexible polymers in good solvents.[25] Herein, the value of α_s decreases for both sets of as-produced star polymers with the increase of arm length, even with values lower than $^1/_3$ found. It decreases from 0.37 for SPE1-1 to 0.23 for SPE1-6 in the SPE1 set and from 0.41 for SPE2-1 to 0.25 for SPE2-6 in the SPE2 set. These α_s data thus also evidence the sphere-like chain conformation of these star polymers. The α_s values lower than $^1/_3$ have also been reported for some high-molecular-weight multiarm star polymers of high arm numbers.[28]

The ρ factor ($\rho = R_g/R_h$) has also been often used as a sensitive parameter to examine polymer chain conformation. Typically, the ρ value is in the range of 1.25−1.37 for linear unperturbed polymers and is 0.775 for rigid spheres of uniform density.[31−33] For some regular star polymers and dendrimers, the ρ value has been found to be about unity.[31−33] Herein, the ρ value was calculated with the use of $R_{g,w}$ and $R_{h,w}$ for the as-produced and purified star polymers in both sets (see Tables 2−4). It can be found that the ρ value is about unity in each set, along with a very slight reduction with the increase of arm length. This further supports the spherical shape of the core−shell structured multiarm star polymers synthesized herein.

Conclusions

We have reported herein the successful "core-first" synthesis of two sets (SPE1 and SPE2) of novel core−shell structured multiarm star polyethylenes through ethylene multifunctional "living" polymerization using homogeneous hyperbranched polyethylenes encapsulating covalently tethered multinuclear Pd chelate catalysts (HPE-Pd-1 and HPE-Pd-2). These star polymers contain a hyperbranched polyethylene core and multiple linear narrow-distributed polyethylene arms having short branch structures. In the synthesis, Pd−diimine catalyst **2** is covalently immobilized onto the hyperbranched polyethylenes (HPE1 and HPE2) bearing pendant acryloyl anchoring sites to render the multinuclear hyperbranched Pd chelate catalysts (HPE-Pd-1 and HPE-Pd-2). At an ethylene pressure of 400 psi and 5 °C, both HPE-Pd-1 and HPE-Pd-2 have been demonstrated to successfully initiate and catalyze the simultaneous multidirectional "living" arm growth from the hyperbranched core to produce the star polymers. The structure of these star polymers is well-definable, with the core size and the average arm number (about 21 and 28 per star for SPE1 and SPE2 sets, respectively) determined by the hyperbranched polyethylenes (HPE1 and HPE2) used for catalyst immobilization, and the narrow-distributed arm length (up to 48 kg/mol synthesized herein with PDI of about 1.0) controlled by tuning ethylene "living" polymerization time. With the as-produced polymers containing some linear low-molecular-weight polymers by mononuclear catalysts, purification has been carried out by GPC fractionation to give rise to purified multiarm star polymers. Study on their dilute solution properties confirms these multiarm star polymers resemble the spherical chain conformation of rigid spheres and high-generation dendrimers. Nearly zero and even negative α values have been found with the increase of the arm length. Intrinsic viscosity of these star polymers has been found to depend primarily on the arm length, while not on the average arm number. Meanwhile, their R_g data and low α_s and ρ values also confirms their unique nanoscaled globular structures.

Acknowledgment. The financial support from the Ontario Ministry of Research and Innovation as an Early Researcher Award (ERA) to Z.Y. is greatly appreciated. The authors also thank the Natural Science and Engineering Research Council (NSERC) of Canada and the Canadian Foundation for Innovation (CFI) for funding research infrastructures. Mr. Wei Liu carried out some experiments on polymer cleavage.

References and Notes

(1) (a) Mishra, M., Kobayashi, S., Eds. *Star and hyperbranched polymers*; Marcel Dekker Inc.: New York, 1999. (b) Inoue, K. *Prog. Polym. Sci.* **2000**, *25*, 453.

(2) (a) Helms, B.; Guillaudeu, S. J.; Xie, Y.; McMurdo, M.; Hawker, C. J.; Fréchet, J. M. J. *Angew. Chem., Int. Ed.* **2005**, *44*, 6384. (b) Chi, Y.; Scroggins, S. T.; Fréchet, J. M. J. *J. Am. Chem. Soc.* **2008**, *130*, 6322. (c) Kanaoka, S.; Yagi, N.; Fukuyama, Y.; Aoshima, S.; Tsunoyama, H.; Tsukuda, T.; Sakurai, H. *J. Am. Chem. Soc.* **2007**, *129*, 12060.

(3) (a) Ooya, T.; Lee, J.; Park, K. *J. Controlled Release* **2003**, *93*, 121. (b) Wang, F.; Bronich, T. K.; Kabanov, A. V.; Rauh, R. D.; Roovers, J. *Bioconjugate Chem.* **2005**, *16*, 397.

(4) Wang, T.-Y.; Tsiang, R. C.-C.; Liou, J.-S.; Wu, J.; Sheu, H.-C. *J. Appl. Polym. Sci.* **2001**, *79*, 1838.

(5) (a) Groll, J.; Amirgoulova, E. V.; Ameringer, T.; Heyes, C. D.; Röcker, C.; Nienhaus, G. U.; Möller, M. *J. Am. Chem. Soc.* **2004**, *126*, 4234. (b) Lupitskyy, R.; Roiter, Y.; Constantinos, T.; Minko, S. *Langmuir* **2005**, *21*, 8591.

(6) Some examples: (a) Hadjichristidis, N.; Pitsikalis, M.; Pispas, S.; Iatrou, H. *Chem. Rev.* **2001**, *101*, 3747. (b) Lee, J. S.; Quirk, R. P.; Foster, M. D. *Macromolecules* **2005**, *38*, 5381. (c) Elkins, C. L.; Viswanathan, K.; Long, T. E. *Macromolecules* **2006**, *39*, 3132. (d) Hirao, A.; Higashihara, T.; Inoue, K. *Macromolecules* **2008**, *41*, 3579.

(7) Some examples: (a) Shohi, H.; Sawamoto, M.; Higashimura, T. *Macromolecules* **1991**, *24*, 4926. (b) Storey, R. F.; Shoemake, K. A.; Mays, J. W.; Harville, S. *J. Polym. Sci., Part A: Polym. Chem.* **1997**, *35*, 3767. (c) Jacob, S.; Majoros, I.; Kennedy, J. P. *Macromolecules* **1996**, *29*, 8631.

(8) Some examples: (a) Wiltshire, J. T.; Qiao, G. G. *Macromolecules* **2006**, *39*, 4282. (b) Trollsàs, M.; Atthof, B.; Wursch, A.; Hedrick, J. L.; Pople, J. A.; Gast, A. P. *Macromolecules* **2000**, *33*, 6423. (c) Trollsàs, M.; Hedrick, J. L.; Mecerreyes, D.; Dubois, Ph.; Jérôme, R.; Ihre, H.; Hult, A. *Macromolecules* **1997**, *30*, 8508. (d) Zhao, Y.; Shuai, X.; Chen, C.; Xi, F. *Macromolecules* **2004**, *37*, 8854. (e) Hedrick, J. L.; Magbitang, T.; Connor, E. F.; Glauser, T.; Volksen, W.; Hawker, C. J.; Lee, V. Y.; Miller, R. D. *Chem.—Eur. J.* **2002**, *8*, 3309. (f) Taton, D.; Feng, X.; Gnanou, Y. *New J. Chem.* **2007**, *31*, 1097.

(9) Some examples: (a) Bazan, G. C.; Schrock, R. R. *Macromolecules* **1991**, *24*, 817. (b) Nomura, K.; Watanabe, Y.; Fujita, S.; Fujiki, M.; Otani, H. *Macromolecules* **2009**, *42*, 899. (c) Beerens, H.; Verpoort, F.; Verdonck, L. *J. Mol. Catal. A: Chem.* **2000**, *159*, 197.

(10) Some examples: (a) Bosman, A. W.; Vestberg, R.; Heumann, A.; Fréchet, J. M. J.; Hawker, C. J. *J. Am. Chem. Soc.* **2003**, *125*, 715. (b) Gao, H.; Ohno, S.; Matyjaszewski, K. *J. Am. Chem. Soc.* **2006**, *128*, 15111. (c) Gao, H.; Matyjaszewski, K. *Macromolecules* **2008**, *41*, 1118. (d) Wiltshire, J. T.; Qiao, G. G. *Macromolecules* **2008**, *41*, 623. (e) Mayadunne, R. T. A.; Jeffery, J.; Moad, G.; Rizzardo, E. *Macromolecules* **2003**, *36*, 1505. (f) Tsoukatos, T.; Pispas, S.; Hadjichristidis, N. *J. Polym. Sci., Part A: Polym. Chem.* **2001**, *39*, 320. (g) Terashima, T.; Kamigaito, M.; Baek, K.-Y.; Ando, T.; Sawamoto, M. *J. Am. Chem. Soc.* **2003**, *125*, 5288. (h) Kim, Y. H.; Ford, W. T.; Mourey, T. H. *J. Polym. Sci., Part A: Polym. Chem.* **2007**, *45*, 4623. (i) Hovestad, N. J.; van Koten, G.; Bon, S. A. F.; Haddleton, D. M. *Macromolecules* **2000**, *33*, 4048. (j) Miura, Y.; Dote, H. *J. Polym. Sci., Part A: Polym. Chem.* **2005**, *43*, 3689. (k) Johnson, J. A.; Finn, M. G.; Koberstein, J. T.; Turro, N. J. *Macromolecules* **2007**, *40*, 3589. (l) Robello, D. R.; André, A.; McCovick, T. A.; Kraus, A.; Mourey, T. H. *Macromolecules* **2002**, *35*, 9334.

(11) See two review articles: (a) Coates, G. W.; Hustad, P. D.; Reinartz, S. *Angew. Chem., Int. Ed.* **2002**, *41*, 2236. (b) Domski, G. J.; Rose, J. M.; Coates, G. W.; Bolig, A. D.; Brookhart, M. *Prog. Polym. Sci.* **2007**, *32*, 30. And some representative examples: (c) Scollard, J. D.; McConville, D. H. *J. Am. Chem. Soc.* **1996**, *118*, 10008. (d) Baumann, R.; Davis, W. M.; Schrock, R. R. *J. Am. Chem. Soc.* **1997**, *119*, 3830. (e) Jayaratne, K. C.; Sita, L. R. *J. Am. Chem. Soc.* **2000**, *122*, 958. (f) Tian, J.; Hustad, P. D.; Coates, G. W. *J. Am. Chem. Soc.* **2001**, *123*, 5134.

(12) (a) Rose, J. M.; Mourey, T. H.; Slater, L. A.; Keresztes, I.; Fetters, L. J.; Coates, G. W. *Macromolecules* **2008**, *41*, 559. (b) Kaneko, H.; Kojoh, S.-I.; Kawahara, N.; Matsuo, S.; Matsugi, T.; Kashiwa, N. *Macromol. Symp.* **2004**, *213*, 335. (c) Kaneko, H.; Kojoh, S.-I.; Kawahara, N.; Matsuo, S.; Matsugi, T.; Kashiwa, N. *J. Polym. Sci., Part A: Polym. Chem.* **2005**, *43*, 5103.

(13) Zhang, K.; Ye, Z.; Subramanian, R. *Macromolecules* **2009**, *42*, 2313.

(14) Concomitant to this work, a most recent ASAP communication by another group reports the synthesis of dendritic polyethylene nanoparticles by chain walking polymerization with multinuclear Pd−diimine catalysts. See: Sun, G.; Guan, Z. *Macromolecules* ASAP article, DOI: 10.1021/ma100367q.

(15) Morgan, S.; Ye, Z.; Zhang, K.; Subramanian, R. *Macromol. Chem. Phys.* **2008**, *209*, 2232.

(16) Johnson, L. K.; Killian, C. M.; Brookhart, M. *J. Am. Chem. Soc.* **1995**, *117*, 6414.

(17) (a) Zhang, Y.; Ye, Z. *Chem. Commun.* **2008**, 1178. (b) Zhang, K.; Ye, Z.; Subramanian, R. *Macromolecules* **2008**, *41*, 640.
(18) Zhang, Y.; Ye, Z. *Macromolecules* **2008**, *41*, 6331.
(19) (a) Ye, J.; Ye, Z.; Zhu, S. *Polymer* **2008**, *49*, 3382. (b) Xiang, P.; Ye, Z.; Morgan, S.; Xia, X.; Liu, W. *Macromolecules* **2009**, *42*, 4946. (c) Morgan, S.; Ye, Z.; Subramanian, R.; Wang, W.-J.; Ulibarri, G. *Polymer* **2010**, *51*, 597.
(20) (a) Guan, Z.; Cotts, P. M.; McCord, E. F.; McLain, S. J. *Science* **1999**, *283*, 2059. (b) Cotts, P. M.; Guan, Z.; McCord, E.; McLain, S. *Macromolecules* **2000**, *33*, 6945. (c) Guan, Z. *Chem.—Eur. J.* **2002**, *8*, 3086.
(21) (a) Ye, Z.; Zhu, S. *Macromolecules* **2003**, *36*, 2194. (b) Ye, Z.; AlObaidi, F.; Zhu, S. *Macromol. Chem. Phys.* **2004**, *205*, 897. (c) Ye, Z.; Li, S. *Macromol. React. Eng.* **2010**, DOI: 10.1002/mren.200900068.
(22) (a) Johnson, L. K.; Mecking, S.; Brookhart, M. *J. Am. Chem. Soc.* **1996**, *118*, 267. (b) Mecking, S.; Johnson, L. K.; Wang, L.; Brookhart, M. *J. Am. Chem. Soc.* **1998**, *120*, 888.
(23) (a) Zhang, K.; Wang, J.; Subramanian, R.; Ye, Z.; Lu, J.; Yu, Q. *Macromol. Rapid Commun.* **2007**, *28*, 2185. (b) Wang, J.; Ye, Z.; Joly, H. *Macromolecules* **2007**, *40*, 6150.
(24) (a) Gottfried, A. C.; Brookhart, M. *Macromolecules* **2001**, *34*, 1140. (b) Gottfried, A. C.; Brookhart, M. *Macromolecules* **2003**, *36*, 3085.
(25) Hiemenz, P. C.; Lodge, T. P. *Polymer Chemistry*, 2nd ed.; CRC Press: Boca Raton, FL, 2007.
(26) Mourey, T. H.; Turner, S. R.; Rubinstein, M.; Fréchet, J. M. J.; Hawker, C. J.; Wooley, K. L. *Macromolecules* **1992**, *25*, 2401.
(27) Lepoittevin, B.; Matmour, R.; Francis, R.; Taton, D.; Gnanou, Y. *Macromolecules* **2005**, *38*, 3120.
(28) Held, D.; Müller, A. H. E. *Macromol. Symp.* **2000**, *157*, 225.
(29) Gauthier, M.; Li, W.; Tichagwa, L. *Polymer* **1997**, *38*, 6363.
(30) Aharoni, S. M.; Crosby, C. R. I.; Walsh, E. K. *Macromolecules* **1982**, *15*, 1093.
(31) Huang, H.-M.; Liu, I.-C.; Tsiang, R. C.-C. *Polymer* **2005**, *46*, 955.
(32) Schappacher, M.; Deffieux, A. *Macromolecules* **2000**, *33*, 7371.
(33) Ishizu, K.; Ono, T.; Uchida, S. *Macromol. Chem. Phys.* **1997**, *198*, 3255.